IOP Conference Series:
Earth and
Environmental Science

PAPER • **OPEN ACCESS**

Ciprofloxacin removal by adsorption-photocatalysis effect of $SrBi_4Ti_4O_{15}$

To cite this article: A Febrianti and A Prasetyo 2025 *IOP Conf. Ser.: Earth Environ. Sci.* **1574** 012006

Ciprofloxacin removal by adsorption-photocatalysis effect of $SrBi_4Ti_4O_{15}$

A Febrianti[1], A Prasetyo[1*]

[1]Department of Chemistry, Faculty Science and Technology, Universitas Islam Negeri Maulana Malik Ibrahim Malang, Jalan Gajayana 50 Malang, 65145 Indonesia

[*]E-mail: anton@kim.uin-malang.ac.id

Abstract. The $SrBi_4Ti_4O_{15}$ compound has been reported to possess photocatalytic properties therefore it can applied to antibiotic waste treatment. In this research, we synthesized the $SrBi_4Ti_4O_{15}$ compound using the molten salt method and then tested its ability to reduce the concentration of ciprofloxacin through adsorption and adsorption-photocatalysis mechanisms. The diffractogram showed that the target sample ($SrBi_4Ti_4O_{15}$) was successfully synthesized; however, impurities in the form of compounds $SrCO_3$, $Na_2Ti_7O_{15}$, $K_2Ti_6O_{12}$ and $Bi_{12}Cl_{14}$ were still detected. The SEM image shows that the sample particles are plate-like in shape; however, agglomeration is still observed. Meanwhile, the Kubelka-Munk equation calculation results showed that the $SrBi_4Ti_4O_{15}$ compound has a band gap energy of 3.14 eV. The ciprofloxacin adsorption test demonstrated a removal efficiency of 64.73% for 90 minutes, while the synergistic adsorption–photocatalysis test achieved a degradation efficiency of 67.57% for 90 minutes. It indicated that the contribution of the photocatalytic mechanism to the reduction of ciprofloxacin concentration is small. It may correlate to high adsorption can inhibit photocatalysis mechanism

Keyword: $SrBi_4Ti_4O_{15}$, adsorption-photocatalysis, ciprofloxacin

1. Introduction

The increase in population has led to a significant rise in pharmaceutical production over the past few decades. Among these, the widespread use of antibiotics can result in the accumulation of hazardous substances in aquatic environments, negatively impacting the health of humans, animals, and plants [1-2]. This extensive use has raised concerns about antibiotic resistance and its effects on human health and ecosystems [3]. Ciprofloxacin is one of the most commonly detected fluoroquinolone antibiotics in wastewater treatment facilities and drinking water sources, often found at significant concentrations [4]. One of the most widely developed methods to address antibiotic wastewater pollution is photocatalysis. This method utilizes light to accelerate chemical reactions with the assistance of a catalyst material. The degradation of ciprofloxacin through photocatalysis involves the generation of reactive species capable of attacking and breaking down ciprofloxacin molecules [5-6].

The enhancement of photocatalytic degradation efficiency can be achieved by combining adsorption and photocatalysis, which may result in a synergistic effect. The adsorption process

allows ciprofloxacin molecules to bind to the catalyst surface prior to light exposure, thereby increasing the concentration of compounds available for reaction with reactive species during photocatalysis [7]. Adsorption refers to the ability of a material to attract and hold molecules from a solution onto its surface. In photocatalytic processes, adsorption plays a crucial role. The synergistic effect between adsorption and photocatalysis occurs because adsorption enables more number of ciprofloxacin molecules to attach to the catalyst surface, thereby increasing the substrate concentration available for the photocatalytic reaction. The more adsorbed molecules, the distance between the ciprofloxacin and the active sites on the catalyst becomes shorter, accelerating the degradation reaction [8]. The synergistic adsorption-photocatalysis effect has been reported by several researchers [8-9]. Feng et al. (2022) demonstrated that the combination of adsorption and photocatalysis significantly improved the removal efficiency of organic pollutants [10].

The photocatalytic mechanism involving adsorption consists of several interacting stages. When a semiconductor material used as a photocatalyst is exposed to UV or sunlight, electron-hole pairs are generated within the semiconductor structure. The excited electrons migrate to the conduction band, while the holes remain in the valence band. The catalyst surface, already loaded with adsorbed pollutants, facilitates interaction between the excited electrons and the pollutants. Adsorption increases the local concentration of pollutants near the photocatalyst surface, accelerating reduction reactions. The generated electrons are capable of reducing pollutants into less harmful substances. The presence of an adsorbent enhances photocatalytic efficiency by improving the interaction between the photocatalyst and the pollutant, as well as promoting faster separation of electrons and holes. Thus the combination of adsorption and photocatalysis can effectively reduce environmental pollution [11]. It showed that the synergistic effect of adsorption-photocatalysis have potency to enhance the photocatalysis activity.

Aurivillius compounds with plate-like morphology have been reported to exhibit good photocatalytic activity. Haikal and Prasetyo (2021) synthesized plate-like $SrBi_4Ti_4O_{15}$ and reported its good photocatalytic in rhodamine B degradation [12]. The plate-like morphology increases the surface area, and providing more active sites for degradation reactions therefore can enhance activity photocatalytic [13]. However the studied about antibiotics removal by $SrBi_4Ti_4O_{15}$ still limited. Therefore, in this research, we synthesized plate-like $SrBi_4Ti_4O_{15}$ by molten salt and studied the effect of adsorption-photocatalysis in ciprofloxacin removal.

2. Material and Methods

2.1 Materials

The materials used in this researh: $SrCO_3$ powder (Sigma-Aldrich, 99.9%), Bi_2O_3 powder (Himedia, 99.9%), TiO_2 powder (Sigma-Aldrich, 99.9%), KCl (Merck, 99.9%), NaCl (Merck, 99.9%), $AgNO_3$ (Merck, 2.3%), ciprofloxacin solution, acetone and distilled water.

2.2 Synthesis of $SrBi_4Ti_4O_{15}$ via the molten salt method

The precursors were mixed with NaCl/KCl salt. The mol salt ratio used was 1:1, and the mol ratio between the sample product and salt was 1:7. Then, precursors and salt were homogenized by grinding in an agate mortar for 1 hour and calcined at 750 and 820°C for 6 hours. After calcination, the sample was washed repeatedly with hot distilled water to remove residual salts. The presence of salt in the product was analysed by adding $AgNO_3$ solution to the filtrate; the formation of a white precipitate indicated the presence of chloride ions. If salt was completely removed so the product was dried in an oven at 90°C for 3 hours [12].

2.3 Characterization of $SrBi_4Ti_4O_{15}$

Characterization technique were used: (a) *X*-ray diffraction (XRD) with Cu Kα radiation (40 kV and 30 mA) over a 2θ range of 10–90°, (b) scanning electron microscope (SEM) with a magnification range of 5.000 to 15.000, (c) ultraviolet (UV)-visible (Vis) diffuse reflectance spectroscopy (DRS) and measured in the wavelength range of 200-800 nm, (d) infrared (IR) spectroscopy instrument within the wavenumber range of 4000–400 cm^{-1}.

2.4 Adsorption-desorption test

The test was conducted on the $SrBi_4Ti_4O_{15}$ catalyst sample. An 80 mL ciprofloxacin stock solution (8 ppm) was placed in a 100 mL measuring cylinder. Then, 80 mg of $SrBi_4Ti_4O_{15}$ catalyst was added. Then the mixture was put into a photocatalytic reactor and stirred for 0, 30, 60, 90, and 120 minutes. Afterward, the mixture was filtered using filter paper to separate the catalyst precipitate from the supernatant. The supernatant was transferred into a cuvette for absorbance measurement using a UV-Vis spectrophotometer.

2.5 Adsorption-photocatalyst test

An 80 mL ciprofloxacin solution (8 ppm) was placed into a 100 mL beaker glass, followed by the addition of 80 mg $SrBi_4Ti_4O_{15}$ catalyst. The mixture was put into the photocatalytic reactor and stirred in the dark for the adsorption-desorption equilibrium time (determined from the adsorption test). Subsequently, the suspension was irradiated using five UV spotlight LED bulbs (Bohlman 80 LEDs, 220 V, E27 commercial UV lamp) for 30, 60, and 90 minutes. After irradiation, the solution was filtered using filter paper to separate the ciprofloxacin solution from the catalyst precipitate. The filtered ciprofloxacin solution was transferred into a cuvette for absorbance measurement using a UV-Vis spectrophotometer. The degradation percentage was calculated to evaluate the relationship between catalyst composition and ciprofloxacin degradation efficiency, using Equation 1.

$$\text{Degradation (\%)} = (C_0 - C_t) / C_0 \times 100\% \quad (1)$$

C_0 is the initial concentration of ciprofloxacin (mg/L) and C_t is the concentration at time *t*.

3. Result and Discussion

3.1 Characterization

The X-ray diffraction (XRD) pattern of the $SrBi_4Ti_4O_{15}$ compound is shown in **Figure 1**. The diffractogram product were identified by matching them with the data from the Joint Committee on Powder Diffraction Standards (JCPDS) No. 00-049-0973 for $SrBi_4Ti_4O_{15}$. The comparison results revealed that several characteristic peaks of $SrBi_4Ti_4O_{15}$ were observed at 2θ (°): 21.72, 23.36, 24.04, 26.1, 27.7, 30.4, 32.9, 36.8, 39.7, 40.5, 47.2, 48.3, 48.9, 51.6, 52.38, 53, and 57. It indicated that $SrBi_4Ti_4O_{15}$ was successfully synthesized. However several additional peaks were detected that did not match the standard pattern that correlate to impurity phases. The impurity phases in sample product i.e. (a) $SrCO_3$ (b) $Na_2Ti_7O_{15}$ (c) $K_2Ti_6O_{12}$, and (d) $Bi_{12}Cl_{14}$.

The XRD diffractogram of the synthesized $SrBi_4Ti_4O_{15}$ compound shows broadened. It indicated that the material possesses a low degree of crystallinity. Peak broadening is typically associated with small crystallite sizes and structural disorder within the crystal lattice. The smaller the crystallite size, the broader the diffraction peaks tend to appear. The high and uneven background in the XRD diffractogram is attributed to the presence of amorphous phases in the

sample, which produce diffuse scattering and consequently increase background intensity. The presence of an amorphous phase reduces the intensity of diffraction peaks and caused further broadening [14].

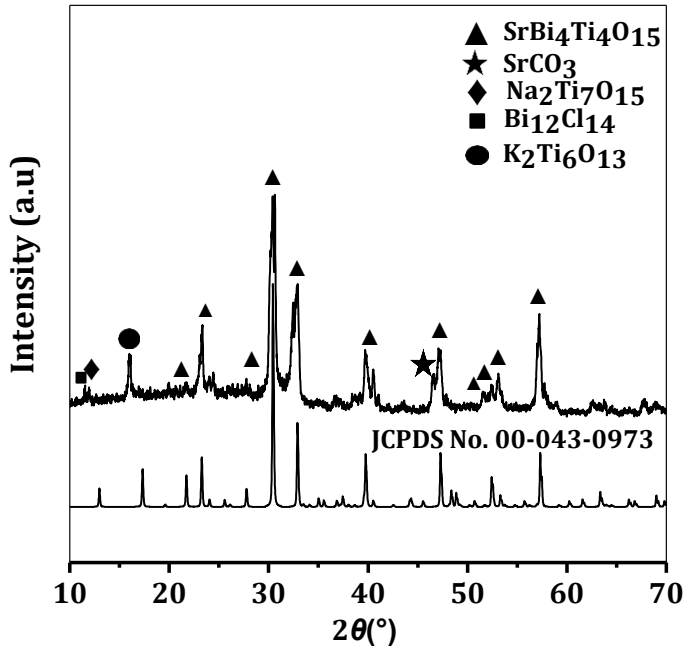

Figure 1. Diffractogram of $SrBi_4Ti_4O_{15}$.

The SEM image and particle size distribution are show in **Figure 2**. The particle morphology exhibits a plate-like structure, which is a characteristic feature of Aurivillius compounds, including $SrBi_4Ti_4O_{15}$ [15-16]. The SEM image also shows a non-uniform particle size distribution, with smaller particles dispersed alongside larger ones. Particle size distribution (**Figure 2b**) indicates surface morphological heterogeneity, where the dominant particle size ranges from 1–2 μm, although larger particles are also present. Particle size is inversely related to specific surface area, where smaller particles provide a larger total surface area. Non-uniform particle size can influence the available active surface area for adsorption processes. A larger surface area offers more active sites for interaction with ciprofloxacin molecules. The smaller particle sizes correlate the high nucleation rate. Marela et al. (2021) reported that at lower synthesis temperatures, higher nucleation rates result in the formation of numerous crystal nuclei within a short time. The formation of many nuclei limits particle growth, leading to smaller overall particle sizes [17].

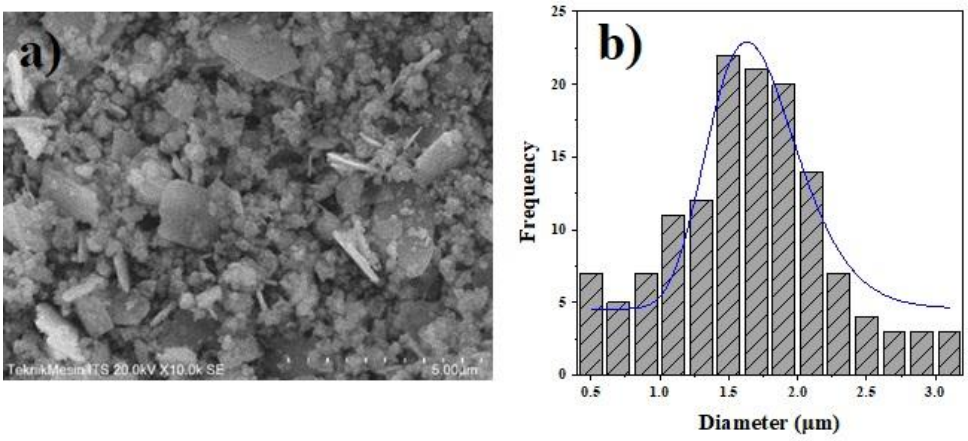

Figure 2. SEM images of $SrBi_4Ti_4O_{15}$ compound at (a) 10,000× magnification and (b) particle size distribution.

The reflectance spectrum of the $SrBi_4Ti_4O_{15}$ compound is shown in **Figure 3a**. The obtained data were processed using the Kubelka–Munk equation to calculate the band gap energy (**Figure 3b)**. Based on the results, the $SrBi_4Ti_4O_{15}$ compound exhibits a band gap energy of 3.14 eV (394.85 nm). Several previous studies have reported similar band gap values for $SrBi_4Ti_4O_{15}$. Al-Abrar et al. (2023) reported that $SrBi_4Ti_4O_{15}$ have band gap energy of 3.14 eV (394.85 nm) [18]. On other hand, Saputra and Prasetyo (2024) also reported that $SrBi_4Ti_4O_{15}$ have band gap energy of 3.14 eV (394.85 nm) [19].

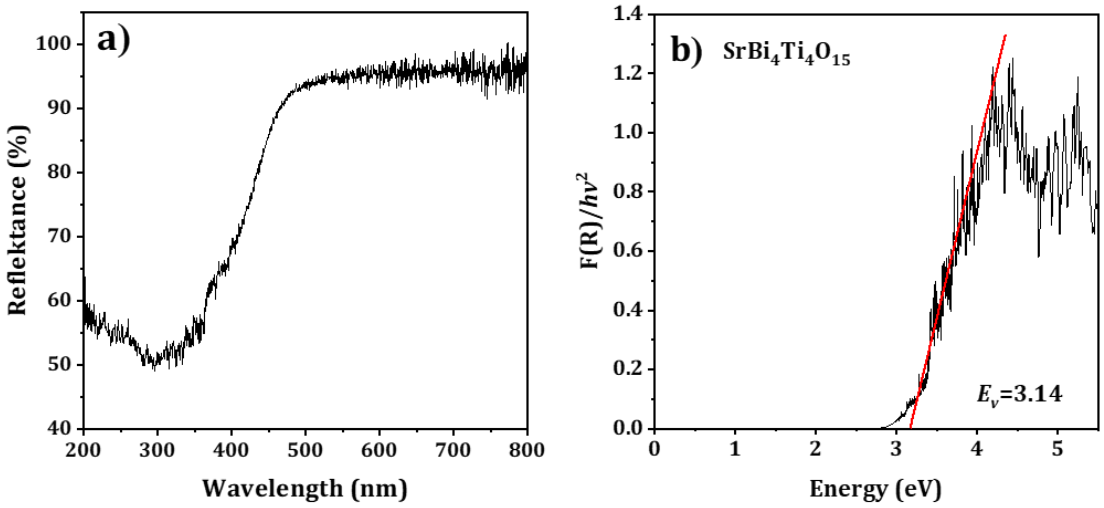

Figure 3. (a) Reflectance spectrum of $SrBi_4Ti_4O_{15}$ compound (b) Tauc plot of $SrBi_4Ti_4O_{15}$ compound.

3.2 Adsorption test of $SrBi_4Ti_4O_{15}$ compound

The results of adsorption test were shown on **Figure 4** and tabulated on **Table 1**. It can be seen that the ciprofloxacin concentration decreases as results the adsorption process. **Figure 4** also showed that the ciprofloxacin concentration decreases was significant up to 90 minutes and then increase again at 120 minutes. It indicated that the adsorption equilibrium time was reached at the 90 minute and caused the desorption/the release of adsorbed molecules from the $SrBi_4Ti_4O_{15}$ surface. Desorption may result from several factors, such as weak physical interactions between the adsorbate and adsorbent, or thermodynamic imbalance at the material's surface. It may also occur when the system reaches saturation and the adsorbate molecules, which are no longer stable on the surface, return to the ciprofloxacin solution due to weak physical forces such as Van der Waals interactions or hydrogen bonding [20]. In addition, the adsorption test results also showed that ciprofloxacin concentration decreases by 64.73% for 90 minutes. Meanwhile, the Aurivillius compound ability as adsorbent for ciprofloxacin has been reported by Saputra and Prasetyo. (2024) [19].

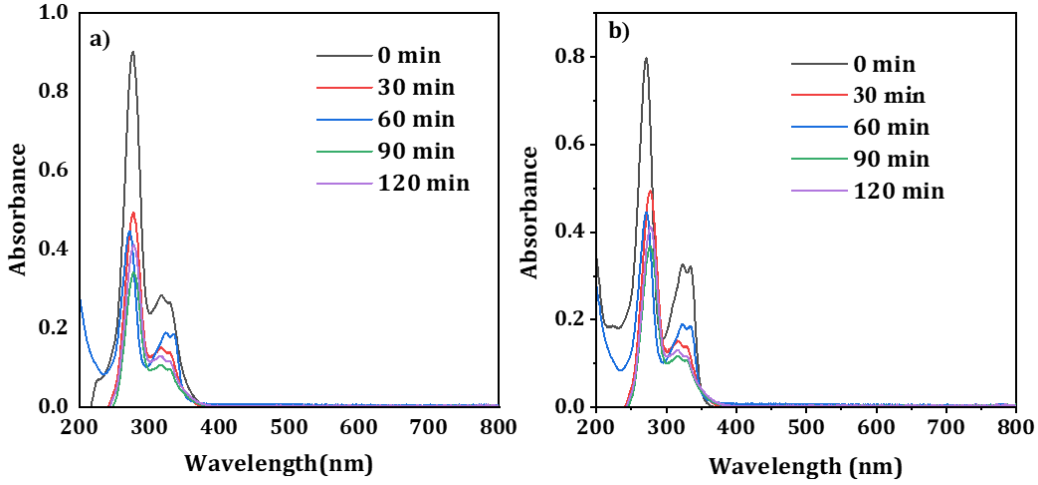

Figure 4. Adsorption test of $SrBi_4Ti_4O_{15}$ compound: (a) 1st test (b) 2nd test.

Table 1. The results of adsorption test.

Time (min)	Experiment 1		Experiment 2	
	Ciprofloxacin concentration (ppm)	Adsorption (%)	Ciprofloxacin concentration (ppm)	Adsorption (%)
30	3.85	48.12	3.97	46.40
60	3.42	53.85	3.45	53.34
90	2.50	66.26	2.72	63.21
120	3.13	57.88	3.32	55.19

3.3 Synergistic adsorption–photocatalytic test using UV light

The results of Adsorption–Photocatalytic test was shown on **Figure 5** and summarized at **Table 2**. It can be seen that the results is slightly higher than adsorption test. It indicated that the adsorption process is more dominant for ciprofloxacin decreases in this research. It may due to the higher adsorption capacity can influence to photocatalysis process. The increasing amount of ciprofloxacin adsorbed may lead to the formation of a thick layer on the photocatalyst surface, which inhibits the penetration of UV light to the active sites of the material, thereby reducing its photocatalytic activity [21].

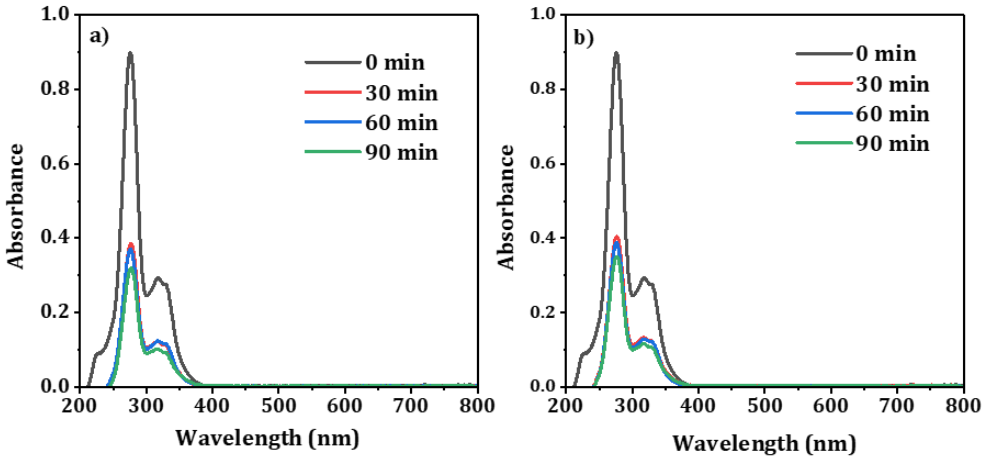

Figure 5. Synergistic adsorption–photocatalytic spectra of $SrBi_4Ti_4O_{15}$: (a) 1st test, and (b) 2nd test.

Table 2. The results of adsorption–photocatalytic test.

Time (min)	Experiment 1		Experiment 2	
	Ciprofloxacin concentration (ppm)	Degradation (%)	Ciprofloxacin concentration (ppm)	Degradation (%)
30	2.90	60.81	2.91	60.81
60	2.76	63.51	2.77	63.51
90	2.31	68.94	2.58	66.21

3.4 IR spectra

IR spectroscopy measurements were carried out on two $SrBi_4Ti_4O_{15}$ samples on: (a) the adsorption test (b) The adsorption–photocatalysis test and IR spectra was shown on Figure 6. The observed peak at 1211.3 and 1151.7 cm^{-1} are associated with the stretching vibrations of aromatic C–F groups, which are characteristic of ciprofloxacin [22]. Meanwhile IR vibration peak at 808.8 cm^{-1} is associated with the stretching vibration of *B*/Ti–O bonds from pseudo perovskite structure (TiO_6 octahedral) [23]. It indicated that the all samples contain $SrBi_4Ti_4O_{15}$ and ciprofloxacin. It

showed that ciprofloxacin is attached to the surface of $SrBi_4Ti_4O_{15}$ that correlates to ciprofloxacin adsorption mechanism.

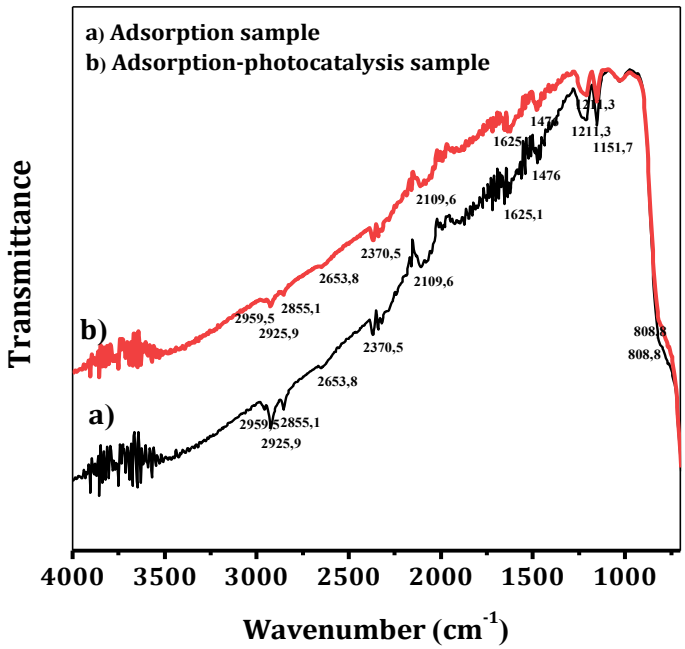

Figure 6. IR spectra of $SrBi_4Ti_4O_{15}$ on (a) adsorption test and (b) adsorption-photocatalysis test.

4. Conclusion

The diffractogram confirmed that $SrBi_4Ti_4O_{15}$ phase was successfully synthesized however the minor impurities still obtained, while SEM images showed the particles morphology of $SrBi_4Ti_4O_{15}$ is plate-like with particle size distribution of 1–2 μm. Kubelka-Munk calculation showed that the $SrBi_4Ti_4O_{15}$ sample have band gap of 3.14 eV. The adsorption test results showed that the $SrBi_4Ti_4O_{15}$ compound has a high ability to adsorb ciprofloxacin (reducing ciprofloxacin concentration by 64% within 90 minutes). However, the high adsorption capacity may reduce its photocatalytic activity performance, so the results of the adsorption–photocatalysis test did not differ much in reducing ciprofloxacin concentration compared to the adsorption test.

References

[1] Abdurahman M H, Abdullah A Z, Shoparwe, N F, 2021 *Chemical Engineering Journal* **413** 127412.
[2] Adhikari S, Lee H H, Kim D H, 2024 *iScience* **27**(9) 110789.
[3] Fei Y, Li Y, Han S, Ma J, 2016 *Journal of Colloid and Interface Science* **484** 196–204.
[4] Ghosh S, Pourebrahimi S, Malloum A, Ajala O J, AlKafaas, S S, Onyeaka H, …and Wani, M Y, 2023 *Materials Today Communications* **37** 107500.
[5] Hayri-Senel T, Kahraman E, Sezer S, Erdol-Aydin N, Nasun-Saygili G, 2024 *Heliyon* **10**(3) e25433.
[6] Jia X, Zhang J, Huang Q, Xiong C, Ji H, Ren Q,…and Ding Y, 2024 *Environmental Research* **241** 117639.
[7] Liu W, He T, Wang Y, Ning G, Xu Z, Chen X,… and Zhao Y, 2020 *Scientific Reports* **10**(1) 11903.
[8] Niño-Torres O, Ramos-Ramírez E, Serafín-Muñoz A, Feria-Reyes R, Carreño-Aguilera G, Cruz-Jiménez G, *Gutiérrez*-Ortega N A, 2024 *Catalysts* **14** 737.

[9] Kusiak-Nejman, E, Sienkiewicz A, Wanag A, Rokicka-Konieczna P, Morawski A W, 2021 *Catalysts* **11** 172.
[10] Feng J, Ran X, Wang L, Xiao, B, Lei L, Zhu J, and Li R, 2022 *International Journal of Molecular Sciences* **23**(22) 14264.
[11] Haleem A, Shafiq A, Chen, S-Q, Nazar, M A, 2023 *Molecules* **28** 1081.
[12] Haikal F, Prasetyo, A, 2021 *al-Kimiya* **8**(1) 37–41.
[13] Chen Z, Hong J, Wuliang J, Chunkai S, 2016 *Applied Catalysis B: Environmental* **180** 698-706.
[14] Veres Á, Ménesi J, Janáky C, Samu G F, Karl M, Xu Q, Salahioglu F, … Zhong Z, 2015 *RSC Advance,* **5,** 2421-2428.
[15] Zhao Z, Li X, Ji H, Deng M, 2014 *Integrated Ferroelectrics* **154(**1) 154-158.
[16] Cahyo I N, Aini N, Steky F V, Suendo V, Safitri W N, Prasetyo A, 2023 *Journal of the Iranian Chemical Society* **20** 3079–3085.
[17] Marela S D, Aini N, Hardian A, Suendo V, Prasetyo A, 2021 *The Journal of Pure and Applied Chemistry Research* **10**(1) 64–71.
[18] Al-Abrar M L, Hastuti E, Prasetyo A, 2023 *Jurnal Rekayasa Kimia & Lingkungan* **17**(2) 182–189.
[19] Saputra B A, Aeni S Q, Hikmah N, Prasetyo A, 2024 *The 14th International Conference on Green Technology, Faculty of Science & Technology*, **14**(1) 1-6.
[20] Gupta V K, Ali I, Saleh T A, Nayak A, Agarwal S, 2012 *RSC Advances* **2**(16) 6380.
[21] Hikmah N, Prasetyo A, 2025 *Neutrino* **17**(2) 81-88.
[22] Tofanello A, Belleti E, Adrianne Brito A M M, Nantes-Cardoso, I L, 2021, Materials Research **24**(6) e20210198.
[23] Hou J, Kumar R V, Qu Y, Krsmanovic D, 2010 Journal of Nanoparticle Research **12** 563-571.